XY antiferromagnetic ordering in $CoCl_2 \cdot 2$(pyrazine) and $CoBr_2 \cdot 2$(pyrazine)

Richard L. Carlin and David W. Carnegie, Jr.
Department of Chemistry, University of Illinois at Chicago, Chicago, Illinois 60680

Juan Bartolomé and Domingo González
Deparmento de Termología, Facultad de Ciencias, Universidad de Zaragoza, 50009 Zaragoza, Spain

Luis M. Floría
Deparmento de Agricultura y Economía, Facultad de Veterinaria, Universidad de Zaragoza, 50013 Zaragoza, Spain

(Received 25 October 1984)

The magnetic susceptibility of polycrystalline samples of $CoCl_2 \cdot 2$(pyrazine) and $CoBr_2 \cdot 2$(pyrazine) has been measured over the temperature interval of 40 mK to 4.2 K. Heat-capacity measurements of the bromide measured between 100 mK and 1 K are also reported. Both compounds order antiferromagnetically at $T_c = 0.855(5)$ K for the chloride and $T_c = 0.66(1)$ K for the bromide. The data above T_c can be adequately fitted to susceptibility and specific-heat predictions calculated with high-temperature series for the $S = \frac{1}{2}$, XY simple cubic antiferromagnet, with exchange constants $J/k - 0.423$ K (Cl) and -0.33 K (Br). Below T_c, a crossover to Ising behavior has been detected.

I. INTRODUCTION

The best magnetic systems approaching the XY-model behavior have been found in compounds of Co^{2+} due to the strongly anisotropic properties of the ground Kramers doublet. At temperatures below 30 K only the ground state is appreciably populated and an effective spin $S' = \frac{1}{2}$ can be assigned to it. This is true whether the cobalt resides in four-coordinate tetrahedral symmetry or six-coordinate octahedral symmetry. The XY characteristics are caused by crystal fields of appropriate symmetry and by the signs of the parameters, as occurs for the distorted tetrahedral coordination, which renders either the $|\pm\frac{3}{2}\rangle$ or the $|\pm\frac{1}{2}\rangle$ doublet as the ground state. Thus, for the XY chain-compound Cs_2CoCl_4 (Ref. 1) the latter doublet is the ground state, with effective-spin Landé factors $g'_{\parallel} = 2.4$ and $g'_{\perp} = 4.8$. In the series $[Co(C_5H_5NO)_6]X_2$ (X=perchlorate, nitrate, fluoborate, or iodide),[2-4] the trigonally distorted octahedron formed by the oxygen atoms of the pyridine N-oxide groups produces a ground doublet with XY anisotropy, corresponding to $g'_{\parallel} = 2.42$ and $g'_{\perp} = 4.99$. Finally, a tetragonal symmetry in the ligand field produced by four O atoms at the equatorial vertices and two Cl atoms at the apical ones of a distorted octahedron causes the XY behavior of $CoCl_2 \cdot 6H_2O$,[5,6] with $g'_{\parallel} = 2.9$ and $g'_{\perp} = 4.9$.

In a previous paper[7] the XY properties of $CoCl_2 \cdot 2$(pyz) [pyz is pyrazine, $N(CHCH)_2N$] were reported as determined by heat capacity measurements. This compound is similar to $CoCl_2 \cdot 6H_2O$, since the Co^{2+} ions are surrounded by tetragonally distorted octahedron with N atoms at the equatorial vertices and two Cl atoms at the apices. This material together with the $[Co(C_5H_5NO)_6]X_2$ series have the additional interest that they provide the only three-dimensional examples of the XY model.

In two previously reported XY systems $CoCl_2 \cdot 6H_2O$[5] and Co(1,2,4-triazole)$_2$(NCS)$_2$,[8] there is a crossover to Ising behavior at low enough temperatures, caused by anisotropy within the XY plane. Thus, from the single-crystal susceptibility measurements, the ratios $g'_x/g'_y = 1.02$ and 1.11 were deduced for the hydrated chloride and the triazole compound, respectively. As such crossover could also occur in the $CoX_2 \cdot 2$(pyz) case it has been probed for this effect. Besides, in a continuing effort to extend the existing spin-wave theory[9] for intermediate anisotropy, predictions for heat capacity and susceptibility have been obtained.

In the present paper powder susceptibility measurements of both $CoCl_2 \cdot 2$(pyz) and $CoBr_2 \cdot 2$(pyz) together with heat capacity data on the latter compound are reported. Moreover, a comparative study including a reanalysis of the previously reported data for $CoCl_2 \cdot 2$(pyz) is performed.

The chloride[10] is tetragonal, $I4/mmm$, and has two molecules in the unit cell. The system is formed by layers of CoN_4Cl_2 units, linked by the pyrazine ligands[7,10] and thus the three-dimensional magnetic character in this polymeric compound appears to be accidental in nature. The likely superexchange paths have been discussed earlier,[7] as well as the justification for applying the three-dimensional simple cubic model to these compounds.

II. EXPERIMENTAL

The experiments were performed on powdered samples because efforts to obtain suitable single crystals were unsuccessful. The compounds were prepared by mixing together solutions of the cobalt halide and pyrazine, obtained commercially. Heat capacity measurements were performed in an adiabatic demagnetization apparatus described elsewhere.[11] Susceptibilities between 1.2 and 4.2 K were measured by a mutual inductance procedure as described earlier,[12] with each data point calibrated against cerium magnesium nitrate (CMN). Measurements below 2 K were performed in a dilution refrigerator and the procedure has been described in detail.[13]

III. RESULTS AND DISCUSSION

A. Heat capacity

The specific heat results for $CoBr_2 \cdot 2(pyz)$ show a sharp peak at $T_c = 0.66 \pm 0.01$ K due to the magnetic ordering. The experimental data are depicted in Fig. 1 together with those for $CoCl_2 \cdot 2(pyz)$ for comparison. The low-temperature tail shows an increase for both compounds, which is a contribution due to the hyperfine interaction between the cobalt electronic and nuclear spins. The small peak observed near 100 mK in the bromide is probably due to loss of thermal contact between the spin and the phonon systems, because the experimental relaxation times were extremely long. Consequently, this feature will be neglected.

Subtracting a AT^{-2} term which represents the hyperfine contribution, a steep slope in the low-temperature magnetic heat capacity is obtained (Fig. 2), which allows extrapolation down to $T=0$ K. The constant A for the asymptotic high-temperature hyperfine contribution is listed for both compounds in Table I and compared to the value obtained for $[Co(apy)_6](ClO_4)_2$, where apy is antipyrine, in which the Co^{2+} ion also exhibits XY anisotropy.[14]

In the high-temperature tail of the $CoBr_2 \cdot 2(pyz)$ data the onset of the phonon contribution is detected in the last few points. To correct for this effect in the calculation of the critical energy and entropy, the experimental points were extrapolated with a T^{-2} term to $T \to \infty$. After subtraction of the above corrections the critical energies and entropies were obtained.

The Heisenberg Hamiltonian capable of describing the exchange interaction between highly anisotropic cobalt ions is, for effective spin $S' = \frac{1}{2}$,

$$H_{ex} = -2 \sum_{\langle l,j \rangle} (J_x S'_{xi} S'_{xj} + J_y S'_{yi} S'_{yj} + J_z S'_{zi} S'_{zj}) , \qquad (1)$$

where the sum is extended to all possible pairs, and J_x, J_y, and J_z are the exchange constants between parallel spin components. From the previously mentioned examples of systems which approach the XY model experimentally $(g'_x \simeq g'_y) = g'_{xy} > g'_z$, one derives the phenomenological condition

$$a = \frac{J_z}{J_{xy}} = \left[\frac{g'_z}{g'_{xy}} \right]^2 \simeq 0.25, \quad \text{where } (J_x \simeq J_y) = J_{xy} .$$

In absence of theory for arbitrary J's, predictions for the limiting models $J_y = J_z = 0$ (Ising), $J_x = J_y, J_z = 0$ (XY), and $J_x = J_y = J_z$ (Heisenberg) on the simple cubic (sc) lattice are given in Table I. One observes an excellent agreement for both compounds with the theoretical predictions for the XY model, the better agreement for the chloride probably being due to the better quality of the data. Moreover, in Table I the critical values for $[Co(C_5H_5NO)_6](NO_3)_2$,[3] which is the best example for that model so far known, are also included and a good agreement is found as well. From T_c the interaction constants $|J_x|/k$ (Cl) $= 0.423$ K and $|J_x|/k$ (Br) $= 0.33$ K have been obtained.

In both compounds the low-temperature asymptotic behavior of the heat capacity departs from the XY model (see Fig. 2) and, instead, it fits nicely to the Ising $S = \frac{1}{2}$ sc model prediction obtained for the same exchange constants.[15] Such a crossover may be related to a small anisotropy in the XY plane as in the previously mentioned examples. The easy axis within the xy plane may be caused by an extra rhombic distortion, by dipolar interaction between the ordered spins, or both effects superimposed. As stated above, such crossover, i.e., an Ising-like decrease in the low-temperature heat capacity tail, has been previously detected.[5,8] However, in those cases the Ising region occurs at higher relative temperature, probably due to the two-dimensional character of the materials studied.

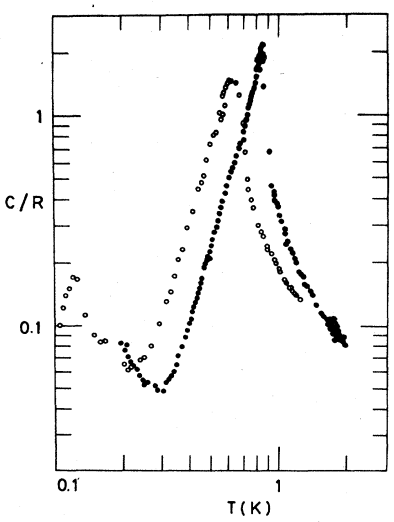

FIG. 1. The measured specific heat of $CoBr_2 \cdot 2(pyz)$ (○) and $CoCl_2 \cdot 2(pyz)$ (●).

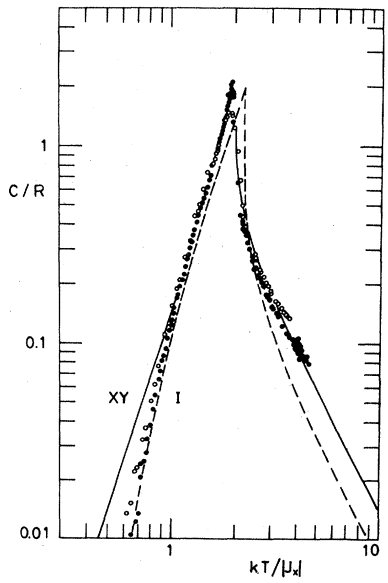

FIG. 2. Data for $CoBr_2 \cdot 2(pyz)$ (○) and $CoCl_2 \cdot 2(pyz)$ (●) plotted against the reduced temperature $k_B T/|J_x|$. The theoretical predictions for the XY and Ising sc $S' = \frac{1}{2}$ models are shown in full and dashed lines, respectively.

TABLE I. Values for $A = C_v T^2/R$ hyperfine constant, and critical energy and entropy parameters.

	$A\times10^{-3}$ (K^2)	T_c(K)	$kT_c/\lvert J_x\rvert$	S_c/R	$(S_\infty - S_c)/R$	$-E_c/RT_c$	$-E_0/RT_c$
Heisenberg, $S=\frac{1}{2}$			1.87	0.48	0.21		
XY, $S=\frac{1}{2}$			2.02	0.44(2)	0.25(1)	0.47(2)	0.78(3)
Ising, $S=\frac{1}{2}$			2.25	0.5579	0.1357	0.2200	0.6651
$[Co(C_5H_5NO)_6](NO_3)_2$		0.458(5)		0.44(2)	0.25(1)	0.45(1)	
$CoBr_2\cdot 2pyz$	2.1(1)	0.66(1)		0.45(2)	0.28(2)	0.49(2)	0.84(2)
$CoCl_2\cdot 2(pyz)$	3.3(1)	0.855(5)		0.45(2)	0.26(1)	0.45(1)	0.81(2)
$[Co(apy)_6](ClO_4)_2$	1.4(1)						

B. Magnetic susceptibility

The susceptibility data sets are reported in Figs. 3 and 4. Broad maxima are observed in each case, with the susceptibility then dropping at lower temperatures. This is the behavior anticipated for a powdered antiferromagnet. The ordering temperatures, taken from the point of maximum slope in the data, are 0.85 ± 0.05 K for the chloride and 0.65 ± 0.05 K for the bromide, in excellent agreement with the transition temperatures measured with heat capacity. Finally, no out-of-phase signal (absorption) was observed, consistent with the absence of any ferromagnetic contributions. Both susceptibility data sets show a small increase at the lowest temperature which may be caused by a small amount of impurity or the experimental difficulties mentioned above.

In the low-temperature tail of the heat capacity, Ising behavior was clearly detected, which implies that there exists a certain anisotropy in the xy plane, giving rise to Ising crossover in the susceptibility as well. Consequently, the $\chi_p(T=0)$ value will decrease strongly, reaching zero for an ideal Ising behavior. Such an effect in the susceptibility has been found in other compounds, for example, in $CoCl_2\cdot 6H_2O$ (quadratic),[5] where the transverse susceptibility behaves Ising-like below T_c, or in $[Co(C_5H_5NO)_6](NO_3)_2$ (sc), where the sharp decrease in χ_{xy} below T_c is argued in terms of a crystalline anisotropy.[4]

C. Effective-spin Hamiltonian

It is known that crystal-field anisotropy produces strongly anisotropic behavior in many Co^{2+} salts. For the compounds reported here, the room-temperature tetragonal symmetry[10] causes the XY character, as detected in $C_p(T)$ and $\chi_p(T)$ measurements, while the crossover to Ising behavior could be due to the influence of a rhombic distortion. To study these two effects the effective spin $S'=\frac{1}{2}$ anisotropic Heisenberg Hamiltonian, which operates on the ground doublet, will be derived. It is equivalent to the true-spin $S=\frac{3}{2}$ Heisenberg Hamiltonian with interaction constant $J(\frac{3}{2})$, including the crystal-field and spin-orbit coupling terms.

The ground state of the free Co^{2+} ion is ^4F ($L=3$, $S=\frac{3}{2}$), which splits due to a cubic crystal field into a singlet Γ_2 and two triplets, Γ_5 and Γ_4, the last being the ground state. The combined effects of spin-orbit coupling and tetragonal, or rhombic distortion split the multiplet into six Kramers doublets. Osaki and Uryû[16] have calculated the anisotropic g factors derived from the ground state in the effective $S'=\frac{1}{2}$ spin formalism, starting from the Hamiltonian

$$H_b = \tfrac{1}{4}B_{T2}Q_2^0 + B_{T4}(Q_4^0 - 7Q_4^4) + \tfrac{1}{4}B_{R2}Q_2^2 - \lambda\sum_i \alpha_i \mathbf{l}_i\cdot\mathbf{s}_i \ , \tag{2}$$

where the first two terms correspond to tetragonal symmetry, the third to rhombic, and the last to spin-orbit coupling.

The wave functions of the lowest Kramers doublet may be written in terms of the $|l_z,s_z\rangle$ base, with effective orbital momentum $l=1$, namely

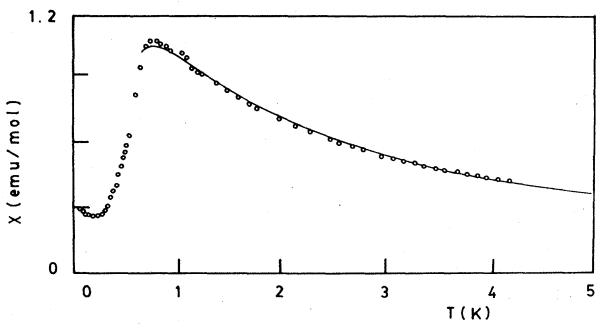

FIG. 3. The zero-field magnetic susceptibility of a polycrystalline sample of $CoBr_2\cdot 2(pyz)$. The curve is the best fit to the data, as described in the text.

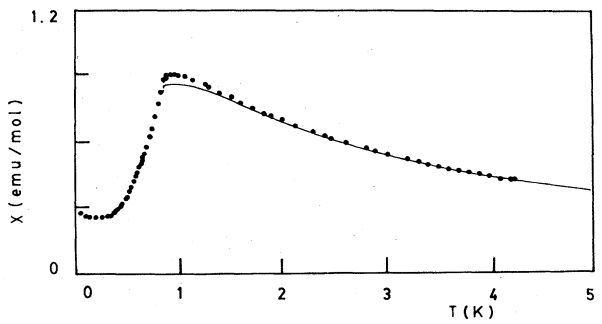

FIG. 4. The zero-field magnetic susceptibility of a polycrystalline sample of $CoCl_2\cdot 2(pyz)$. The curve is the best fit to the data, as described in the text.

$$\phi_{\pm 1/2}=C_1\,|\mp 1,\pm\tfrac{3}{2}\rangle+C_2\,|\mp 1,\mp\tfrac{1}{2}\rangle+C_3\,|\pm 1,\pm\tfrac{3}{2}\rangle$$
$$+C_4\,|\pm 1,\mp\tfrac{1}{2}\rangle+C_5\,|0,\pm\tfrac{1}{2}\rangle+C_6\,|0,\mp\tfrac{3}{2}\rangle\ .$$

Following Lines's[17] notation $S_x=2pS'_x, S_y=2qS'_y$ and $S_z=2rS'_z$, one may obtain the relation between the true-spin $S=\frac{3}{2}$ operators and the effective-spin S' ones, where

$$p=2\sqrt{3}(C_1C_4+C_2C_3+C_5C_6)+4C_2C_4+2C_5^2\ ,$$
$$q=2\sqrt{3}(C_1C_4+C_2C_3-C_5C_6)-4C_2C_4+2C_5^2\ ,$$
$$r=3(C_1^2+C_3^2-C_6^2)-C_2^2-C_4^2+C_5^2\ .$$

Substituting the spin operators in the Heisenberg exchange interaction Hamiltonian one obtains Eq. (1), with $J_x=4p^2J(\frac{3}{2})$, $J_y=4q^2J(\frac{3}{2})$, and $J_z=4r^2J(\frac{3}{2})$.

For the tetragonal case that yields $g_x=g_y>g_z$, as derived from experiment, the condition $C_2=C_3=C_6=0$ is fulfilled, implying $p=q$ and $J_x=J_y$, as expected. The presence of an orthorhombic distortion breaks down the condition and therefore $p\neq q$ and $J_x\neq J_y\neq J_z$.

Therefore, the only variable parameters are then reduced to J_x, B_{T2}, B_{T4}, and B_{R2}, since $Dq=1100\ \mathrm{cm}^{-1}$ and $\lambda=-180\ \mathrm{cm}^{-1}$ (Ref. 18) are considered fixed to the values found for the Tutton salt and the free-ion value, respectively.

For the tetragonal case, the high-temperature (HT) magnetic susceptibility may now be fitted. The reduced susceptibility, defined as

$$\bar{\chi}_i=\frac{\chi_i J_x}{Ng_i^2\mu_B^2}$$

may be calculated in some cases, namely for $\bar{\chi}_{xy}(a=0)$ using HT series expansion for the transverse susceptibility[19] and for $\bar{\chi}_z(a)$ by means of the extended series for the longitudinal susceptibility.[20] They may be combined for a powder according to

$$\chi_p=(N\mu_B^2/J_x)(g_z^2\bar{\chi}_z/3+2g_{xy}^2\bar{\chi}_{xy}/3)\ . \tag{3}$$

The exchange constant J_x is fixed to the value obtained from the heat capacity T_c and the XY model prediction. Furthermore, for every set of B_{T2}, B_{T4}, and $B_{R2}=0$, the parameters g'_{xy} and g'_z are calculated [Eq. (19), Ref. 18], as well as the ratio $a=r^2/p^2$, and substituted in Eq. (3). Hence, the only fitting parameters are those from the crystal-field Hamiltonian B_{T2} and B_{T4}. One notes that the case $B_{T2}>0$ gives XY character, while $B_{T2}<0$ produces Ising anisotropy.

The comparison of the data with the theoretical predictions is shown in Figs. 3 and 4. The precision of the theoretical curve near $\chi_{\max}$ rapidly decreases because of the direct series expansion used in the calculations.

The best fit for both compounds is obtained for $B_{T2}=220\ \mathrm{cm}^{-1}$ and $B_{T4}=5\ \mathrm{cm}^{-1}$. For the bromide compound the anisotropic g' factors are $g'_{xy}=5.77$ and $g'_z=1.90$, the fit being rather good for $T>T_{\max}$ (see Fig. 3). For the chloride case, and maintaining the same g'_{xy}/g'_z ratio, it was necessary to arise the g' factors by 4% to obtain a similar fit as above (see Fig. 4). In both cases it is clear that $g'_{xy}>g'_z$, yielding $a=0.257$ as corresponds to the XY model behavior expected from the specific heat.

The average $\langle g'\rangle=\frac{1}{3}(2g'^2_{xy}+g'^2_z)^{1/2}$ factors are 5.01 and 4.84, for chloride and bromide compounds, respectively, which are somewhat higher than those found in other cobalt compounds. In order to confirm the accuracy of the reported values replicate measurements against CMN were made, but it would still be desirable to have an independent confirmation of the g' values obtained using the EPR technique.

Notwithstanding this fact, it is interesting to note that the mixed valent complex

$$(H_2O)_2Co(II)[(OH)_2Co(III)(en)_2]_2(S_2O_6)_2\cdot 5H_2O\ ,$$

which has $g'_x=5.2$ $g'_y=5.8$, $g'_z=2.3$, and a rather high value of $\langle g'\rangle=4.69$, corresponds also to an XY anisotropic ion.[21] The parameters used to fit the high temperature susceptibility and the EPR spectra are stated in Table II and are of the same order of magnitude as in the present case, though with an orthorhombic distortion.

It cannot be excluded that the approximation made in considering the pure $\bar{\chi}_{xy}(a=0)$ may cause the anomalously high values of the g' parameters, but series for general a are not available. In any case, since $g'_{xy}\gg g'_z$, which implies $J_{xy}\gg J_z$, the XY model applied to the heat capacity for $T>T_c$ is justified.

D. XY—Ising crossover spin-wave theory

The theory may now be extended, including a small orthorhombic distortion on the predominant XY Hamiltonian, i.e., $J_x>J_y\gg J_z$ equivalent to $p>q\gg r$. The Hamiltonian obtained is

$$H_{\mathrm{ex}}=-2J_{\mathrm{av}}\sum_{\langle i,j\rangle}[(1+\theta)S'_{xi}S'_{xj}+(1-\theta)S'_{yi}S'_{yj}]\ , \tag{4}$$

where $J_{\mathrm{av}}=(J_x+J_y)/2$ and $\theta=(p^2-q^2)/(p^2+q^2)$. Thus, the parameter $\theta=0$ corresponds to the pure XY case, while for $\theta>0$ the x axis becomes "easy" within the xy plane. Although this form of the Hamiltonian is very convenient for spin-wave perturbational calculations, in the present context the results will be parameterized in terms of J_x.

The equation of motion of the spin raising and lowering operators, after the application of Fourier transform to Hamiltonian (4), is obtained as

$$i\hbar\dot{S}^{\pm}_k=-J_xzN^{-1}\hbar\Big\{[(1-\theta)/(1+\theta)]\times\sum_q i\gamma_q(2S_qS_{q-k}-i\hbar S_k)+\sum_q\gamma_{k-q}(2S_qS_{k-q}+\hbar S_k)\Big\}\ .$$

If the spin-wave approximations

$$S^{\pm}_K\simeq(2SN)^{1/2}b^{\mp}_{\pm k},\quad S^x_k\simeq NS\delta_{k0}-\sum_r b_r^+b_{r+k}$$
$$S^z_K\simeq\tfrac{1}{2}(2SN)^{1/2}(b_k^-+b_k^+)$$

and $iS^y_k\simeq\frac{1}{2}(2SN)^{1/2}(b_k^--b_k^+)$ are used, the dispersion relation

$$\hbar\omega_k = 2zJ_xS[1-\gamma_k(1-\theta)/(1+\theta)] \quad (5)$$

is obtained, where $\gamma_k = z^{-1}\sum_\delta e^{ik\delta}$.

It is clear that (5) reduces to the Semura and Huber prediction for the pure XY model when $\theta=0$,[22] that is

$$\hbar\omega = 2zJ_xS(1-\gamma_k)^{1/2} .$$

The low-temperature heat capacity is then calculated using (5) and integrating over the whole Brillouin zone. The curves obtained are depicted in Fig. 5 for different θ values. For $\theta=0.2$ there exists already a strong deviation from the XY behavior towards the Ising one and for $\theta=0.5$ an overlap with the Ising prediction is obtained. Therefore, the Ising character is more pronounced for intermediate anisotropic values than the XY one, as could be conjectured from the critical behavior of an intermediate I-XY system. This feature has been previously reported[23] for the $2d$ square lattice case where an almost constant value of the susceptibility critical exponent γ is obtained for $0.25<\theta<1$, and probably for even smaller θ values.

The crossover parameter θ induced by the orthorhombic distortion may be calculated in terms of the corresponding crystal-field coefficient B_{R2}. The values of the parameters B_{T2} and B_{T4} are fixed to their HT determinations tabulated in Table II. Thus, for $B_{R2}=20$ cm^{-1} one obtains $\theta=0.358$, while $J_z/J_x=0.179$ and $g_x'=6.98$, $g_y'=4.43$, and $g_z'=1.86$, i.e., a rhombic perturbation of about 10% of the tetragonal potential produces a strong uniaxial anisotropy in the xy plane, favoring the x axis as easy for $B_{R2}>0$, while the z axis remains "hard."

Consequently, the value of θ needed to fit the low-temperature heat capacity data, $0.3<\theta<0.4$, can be explained. However, we are not aware of the existence of any structural transition in the disordered phase, which would give rhombic symmetry to the system. This point should be further investigated.

On the other hand, it is probable that the effective (XY-I) anisotropy is enhanced by dipolar interactions, which become more important as the sublattice magnetization increases when lowering the temperature, especially in the temperature range involved ($T<300$ mK). We refrain from pursuing this subject further because of lack of knowledge on the ordered magnetic structure.

The low-temperature magnetic susceptibility deviates strongly from the XY model. Indeed, in both cases the limiting experimental value as $T\to 0$ is much lower than the predicted values $\chi_p(T=0,\mathrm{Cl})=0.916$ emu/mol and $\chi_p(T=0,\mathrm{Br})=1.093$ emu/mol. These values have been calculated using (3) with $\bar{\chi}_{xy}(T=0)=0.03887$ (see the Appendix, $\theta=0$ case), $\bar{\chi}_z(T=0)=0.08333$,[24] and the tabulated g_x' and J_x/k parameters, while χ_{tip} has been assumed negligible.

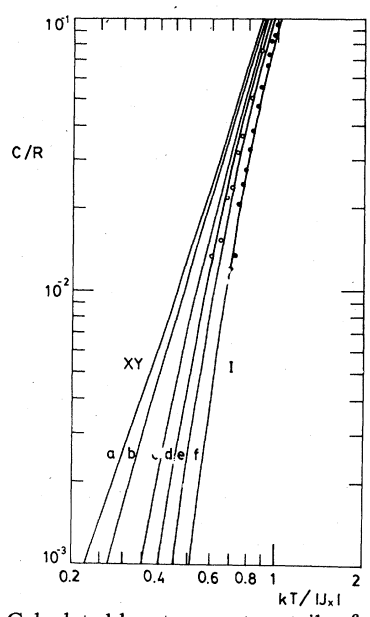

FIG. 5. Calculated low-temperature tails of the heat capacity for different θ values, versus reduced temperature $k_BT/|J_x|$. $CoBr_2\cdot 2(pyz)$ (○) and $CoCl_2\cdot 2(pyz)$ (●) data are included. *a*. $\theta=0$; *b*, $\theta=0.01$; *c*, $\theta=0.05$; *d*, $\theta=0.1$; *e*, $\theta=0.2$; *f*, $\theta=0.5$, coinciding with $\theta=1$.

It may be shown that the XY-I crossover is also manifest in the present low-temperature susceptibility measurements. To analyze this assertion, let us invoke the molecular field theory. For a general anisotropic exchange interaction and imposing an easy xy plane, it follows that

$$\chi_p(T=0)=N\mu_B^2/J_x(\tfrac{1}{3}g_z'^2\bar{\chi}_z+\tfrac{1}{3}g_{xy}'^2\bar{\chi}_{xy}) \quad (6)$$

since the system will flop perpendicular to any applied field in the easy plane. On the other hand, if the presence of an extra anisotropy produces an easy axis in the x direction, then (6) reduces to

$$\chi_p(T=0)=(N\mu_B^2/36J_x)[g_z'^2/(1+J_z/J_x) + g_{xy}'^2/(1+J_y/J_x)] .$$

To reproduce the experimental value χ_p ($T=0$, Cl) $\simeq 0.29$ emu/mol a rhombic distortion $B_{R2}\simeq 40$ cm^{-1} is necessary, which is twice the one needed to explain the heat capacity. Nevertheless, it is evident that again the

TABLE II. Fit parameters and derived values of g_i' and a obtained from $x_p(T)$, in the tetragonal symmetry (A), and considering an orthorhombic distortion (B). The units of the B_i parameters are cm^{-1}.

	$\lvert J_x\rvert/k,K$	B_{T2}	B_{T4}	B_{R2}	g_x'	g_y'	g_z'	$a=\lvert J_z/J_x\rvert$
(A) $CoCl_2\cdot 2(pyz)$	0.423	220	5	0	5.98		1.97	0.257
$CoBr_2\cdot 2(pyz)$	0.33	220	5	0	5.77		1.9	0.257
(B) $CoBr_2\cdot 2(pyz)$		220	5	20	6.98	4.43	1.86	0.179
$\{(H_2O)_2Co[(OH)_2Coen_2]_2\}(S_2O_6)_2\cdot 5H_2O$		100	0.83	30	5.8	5.2	2.3	

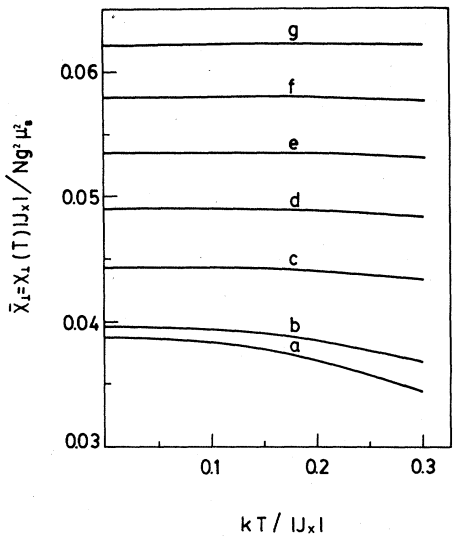

FIG. 6. Calculated $\chi_\perp(T)$ for different θ values versus reduced temperature. *a*, $\theta=0$; *b*, $\theta=0.01$; *c*, $\theta=0.1$; *d*, $\theta=0.2$; *e*, $\theta=0.3$; *f*, $\theta=0.4$; *g*, $\theta=0.5$.

crossover from *XY* to Ising is the cause of the strong decrease in the low-temperature susceptibility. Moreover, the nearly constant dependence of $\chi_\perp(T)$ calculated from spin-wave theory (see the Appendix) explains the flat, low-temperature dependence observed in both experiments.

Finally, it is interesting to observe that, despite the much larger size of the bromide ion, the (presumably isostructural) bromide salt orders at a temperature slightly lower than that of the chloride. Thus the increase in polarizability of bromide over chloride is an important factor in determining the strength of the superexchange path here, and almost completely compensates for the larger Co-Co distances expected for the bromide. Though chloride salts commonly order at lower temperatures than the corresponding bromide, the results reported here are not unique. Thus, $NiCl_2\cdot 2H_2O$ orders at 7.258 K while $NiBr_2\cdot 2H_2O$ orders at 6.23 K,[25] the recently discovered cyclohexylammonium copper (CHAC) salts[26] order at 2.214 K (CHAC-Cl) and 1.50 K (CHAC-Br). Other factors than size and polarizability of course also enter into the determination of T_c; these factors include small variations in both lattice dimensionality and anisotropy, as well as variations in bond angles

ACKNOWLEDGMENTS

The samples were prepared by Rachel Carlin. The authors benefited from discussions with Professor R. Navarro. Experimental help from the Kamerlingh Onnes Lab., Leiden, The Netherlands, is acknowledged. This research was supported by the Solid State Chemistry Program, Division of Materials Research of the National Science Foundation, Grant DMR-8211237 and by the Comisión Asesora de Investigación Científica y Técnica, Grant 3380-83.

TABLE III. Calculated spin reduction ΔS, renormalization factor, i, and $\chi_\perp$ at $T=0$ K, for different values of the θ parameter.

θ	ΔS	i	$\chi_\perp=\chi(T=0)\,\lvert J_x\rvert/Ng_y^2\mu_B^2$
0.0	0.022	−0.0249	0.03887
0.01	0.019	−0.0236	0.03956
0.1	0.009	−0.0154	0.04429
0.2	0.005	−0.0098	0.04900
0.3	0.003	−0.0063	0.05351
0.4	0.0016	−0.0039	0.05792
1.0			0.08333

APPENDIX: CROSSOVER THEORY OF $\chi_\perp(T)$

For the sake of completeness the perpendicular susceptibility will be calculated as a function of temperature. Let H_0 be an external field, parallel to the *xy* plane and perpendicular to the easy axis *x*. At equilibrium the balance of torque gives

$$\phi\simeq H_0/2H_e\ ,$$

where H_e is the effective exchange field, and ϕ is the angle between the sublattice magnetization and the easy axis. Thus, the perpendicular susceptibility takes the form

$$\chi_\perp=2M_s\sin(\phi)/H_0=M_s/H_e\ ,$$

M_s being the magnetization.

The use of the temperature renormalization factor, $i(T)$,[27] defined as

$$S(T)=S(0)[1-i(T)]$$

and

$$H_e(T)=\{2J_xSz/[(1+\theta)g_y\mu_B]\}[1-i(T)] \tag{A1}$$

yields

$$\chi_\perp(T)=(Ng_y^2\mu_B^2/J_x)[(1+\theta)/4z]\times\{[1-\Delta S(T)/S]/[1-i(T)]\}\ ,$$

where $\Delta S(T)$ is the spin reduction at temperature T. If the internal energy is evaluated and compared with the same magnitude obtained using (5), the $i(T)$ value for the *XY* to Ising crossover is easily obtained, namely

$$i(T)=1-\left\{1+(2NS)^{-1}\sum_k[2-\gamma_k(1-\theta)/(1+\theta)]-(NS)^{-1}\sum_k\{(2\langle n_k\rangle+1)[1-\gamma_k(1-\theta)/(1+\theta)]\}\right\}^{1/2}\ ,$$

where the temperature dependence is contained in the Bose distribution function $\langle n_k\rangle$. The spin reduction $\Delta S(T)$ is then given by

$$\Delta S(T)=N^{-1}\sum_{K}\{-\tfrac{1}{2}+[2-\gamma_k(1-\theta)(1+\theta)]/4[1-\gamma_k(1-\theta)/(1+\theta)]^{1/2}\}(1+2\langle n_k\rangle)\ .$$

After that, $\chi_\perp(T)$ is straightforwardly obtained and it is plotted in Fig. 6 for several θ values, and the values for $\Delta S(0)$, $i(0)$, and $\chi_\perp(0)$ are listed in Table III.

[1]H. A. Algra, L. J. de Jongh, H. W. J. Blöte, W. J. Huiskamp, and R. L. Carlin, Physica B **82**, 239 (1976).

[2]H. A. Algra, L. J. de Jongh, W. J. Huiskamp, and R. L. Carlin, Physica B **83**, 71 (1976).

[3]J. Bartolomé, H. A. Algra, L. J. de Jongh, and R. L. Carlin, Physica B **94**, 60 (1978).

[4]A. van der Bilt, K. O. Joung, R. L. Carlin, and L. J. de Jongh, Phys. Rev. B **24**, 445 (1981).

[5]J. W. Metselaar, L. J. de Jongh, and D. de Klerk, Physica B **79**, 53 (1975).

[6]R. L. Carlin, J. Appl. Phys. **52**, 1993 (1981).

[7]D. González, J. Bartolomé, R. Navarro, F. J. A. M. Greidanus, and L. J. de Jongh, J. Phys. (Paris) **39**, C6-762 (1978).

[8]D. W. Engelfriet, W. L. Groeneveldt, H. A. Groenendijk, J. J. Smit, and G. M. Nap, Z. Naturforsch. **35a**, 115 (1980).

[9]R. Navarro and L. J. de Jongh, Physica B **94**, 67 (1978); J. A. Puértolas, R. Navarro, F. Palacio, J. Bartolomé, D. González, and R. L. Carlin, J. Mag. Mag. Mat. **31-34**, 1243 (1983).

[10]P. W. Carreck, M. Goldstein, E. M. McPartlin, and W. D. Unsworth, Chem. Commun. 1634 (1971).

[11]H. A. Algra, L. J. de Jongh, W. J. Huiskamp, and R. L. Carlin, Physica B **92**, 187 (1977).

[12]J. N. McElearney, D. B. Losee, S. Merchant, and R. L. Carlin, Phys. Rev. B **7**, 3314 (1973); S. N. Bhatia, R. L. Carlin, and A. Paduan Filho, Physica B **92**, 330 (1977).

[13]A. van der Bilt, K. O. Joung, R. L. Carlin, and L. J. de Jongh, Phys. Rev. B **22**, 1259 (1980).

[14]H. A. Algra, F. J. A. M. Greidanus, L. J. de Jongh, W. J. Huiskamp, and J. Reedijk, Physica B **83**, 85 (1976).

[15]H. A. Algra, J. Bartolomé, L. J. de Jongh, and R. L. Carlin, Physica B **93**, 114 (1973); M. F. Sykes, D. L. Hunter, D. S. McKenzie, and B. R. Heap, J. Phys. A **5**, 667 (1972).

[16]K. Osaki and N. Uryû, J. Phys. Soc. Jpn. **40**, 1575 (1976).

[17]M. E. Lines, Phys. Rev. **131**, 546 (1963).

[18]A. Abragam and M. H. L. Pryce, Proc. R. Soc., London Ser. A **206**, 173 (1951).

[19]D. J. Austen and D. D. Betts, Phys. Lett. **53A**, 313 (1975); J. Rogiers, D. D. Betts, and T. Lookman, Can. J. Phys. **56**, 420 (1978).

[20]I. M. Kim and M. H. Lee, Phys. Rev. B **19**, 5815 (1979); T. Obokata, I. Ono, and T. Oguchi, J. Phys. Soc. Jpn. **23**, 516 (1967).

[21]H. Kobayashi, K. Ohki, I. Tsujikawa, K. Osaki, and N. Uryû, Bull. Chem. Soc. Jpn. **49**, 1210 (1976).

[22]J. S. Semura and D. L. Huber, Phys. Rev. B **7**, 2154 (1973).

[23]T. Ishikawa and T. Oguchi, J. Phys. Soc. Jpn. **31**, 1021 (1971).

[24]M. E. Fisher, J. Math. Phys. **4**, 124 (1963).

[25]R. L. Carlin and A. J. van Duyneveldt, *Magnetic Properties of Transition Metal Compounds* (Springer, New York, 1977).

[26]K. Kopinga, A. M. C. Tinus, and W. J. M. de Jonge, Phys. Rev. B **25**, 4685 (1982).

[27]F. Keffer, *Encyclopedia of Physics XVIII,* (Springer, New York, 1966), Part 2, p. 109ff.